PAPER

NJC www.rsc.org/njc

Anion recognition and redox sensing by a metalloporphyrin–ferrocene–alkylammonium conjugate†

Christophe Bucher,* Charles H. Devillers, Jean-Claude Moutet,* Guy Royal and Eric Saint-Aman

Laboratoire d'Electrochimie Organique et de Photochimie Rédox (CNRS UMR 5630), Institut de Chimie Moléculaire de Grenoble (CNRS FR 2607), Université Joseph Fourier, BP 53, 38041 Grenoble cédex 9, France

Received (in Toulouse, France) 2nd August 2004, Accepted 10th September 2004
First published as an Advance Article on the web 17th November 2004

The synthesis and characterization of a novel redox molecular receptor is reported. This chemosensor is structured on a ferrocene fragment whose cyclopentadienyl moieties have been connected to distinct and complementary zinc porphyrin and alkylammonium binding sites, enabling multipoint recognition and detection of anionic species. Cumulative effects of multiple anchoring points on this ammonium–ferrocene–metalloporphyrin chemosensor allowed the unprecedented ferrocene-based voltammetric sensing of halide anions.

Introduction

The design of molecular architectures able to electrochemically sense anions is a particularly challenging task. The complexity of such an undertaking unambiguously arises from the necessity to combine different but interacting complexing and signalling units in one unique molecular material.[1] In practice, a host–guest type recognition event has to be "seen" by an internal redox probe through the perturbation of its electrochemical activity. Although most anion binding events greatly suffer from their solvent- and pH-sensitive nature, complexation of negatively charged species in artificial receptors is generally achieved through hydrogen bonding, electrostatic interactions, or coordination to a metal cation.[2] Most of the redox active receptors described in the literature involve only one of these binding modes at a time and the anion complexation in close proximity to the redox-active fragment allows electrochemical detection of the substrate.

In order to improve both recognition and detection ability of chemosensors, we turned our attention towards molecular systems combining multiple complementary binding sites and redox-active reporters. A multipoint molecular recognition event could then be followed and signalled by different redox-active probes distributed at strategic locations on the receptor. The electrochemical, spectroscopic and chemical features of ferrocene–porphyrin conjugates make them outstanding candidates to reach such a goal.[3] Besides the high chemical stability, the well-defined redox characteristics and chemical versatility of both ferrocene and porphyrin fragments, the generation of cationic species upon electrochemical oxidation of both redox moieties is moreover favourable to a strengthening of the anion-receptor interactions and thus to efficient electrochemical recognition of anionic species.

Here, we report the synthesis and characterization of a new electrochemical chemosensor $[\mathbf{1}]^+$ enabling multipoint recognition and detection of anionic species (Fig. 1). This receptor is structured on a ferrocene fragment whose cyclopentadienyl moieties have been connected to distinct and complementary binding sites. On one side an alkylammonium group, known to bring about efficient electrochemical recognition properties in ferrocene-based receptors,[4] has been introduced to promote favourable electrostatic interactions with anionic substrates. The opposing cyclopentadienyl ring has likewise been intimately connected to the π-electronic system of a zinc porphyrin, whose electron-deficient orbitals allow the axial coordination of nucleophilic species.[5] Along with the effective electrochemical sensing of oxoanions, we show that the cumulative effect of multiple anchoring points allows the unprecedented ferrocene-based electrochemical sensing of halide anions.

Results and discussion

Synthesis

The synthesis of the ferrocene–porphyrin receptor $[\mathbf{1}]^+\cdot BF_4^-$ (Scheme 1) started with the mono-protection of diformyl ferrocene **7**[6] according to a literature procedure[7] to give **6** in 70% yield. The acid-catalyzed (TFA) MacDonald-type condensation of the latter with pyrrole and *p*-tolualdehyde in dichloromethane, followed by oxidation with chloranil, afforded a mixture from which **5** could be isolated with 10% yield. **4** was obtained from **5** by removal of the cyclic dithioketal using Ag^+ ions and *N*-chlorosuccinimide (NCS) as the oxidizing agent.[7] A nitrogenous "tail" was then introduced onto the ferrocene moiety by reaction of *n*-hexylamine in anhydrous THF with the regenerated formyl group to produce **3** in good yield. Insertion of zinc(II) into the macrocyclic cavity

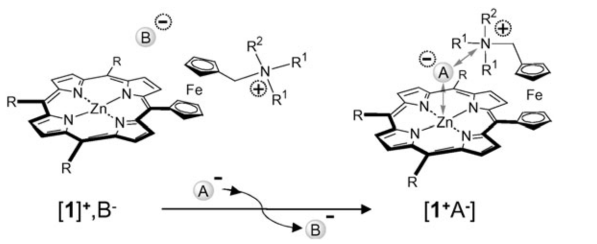

Fig. 1 Cooperative interactions between an anion (A^-) and the ferrocene–ammonium–porphyrin $[\mathbf{1}]^+B^-$ (R: Tol, R^1: Me, R^2: Hexyl).

† Electronic supplementary information (ESI) available: HMQC and COSY of **2**. See http://www.rsc.org/suppdata/nj/b4/b411870g/

DOI: 10.1039/b411870g

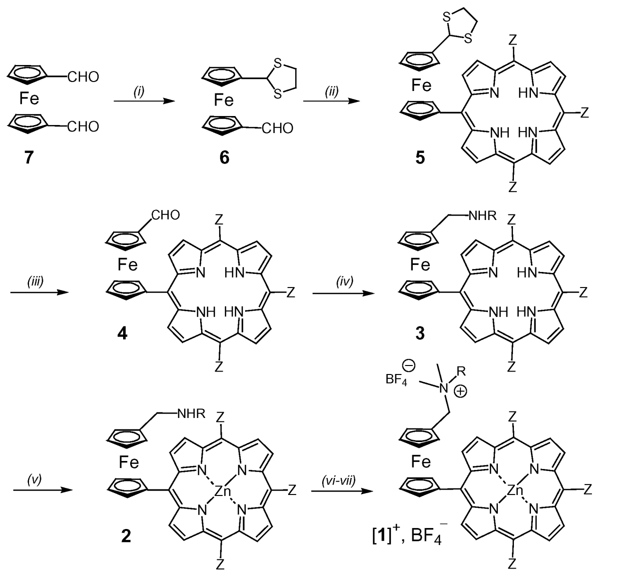

Scheme 1 *Reagents and conditions*: (*i*) 70% yield, CH_2Cl_2, Ar, $SH(CH_2)_2SH$, $BF_3 \cdot OEt_2$, col. chromat. (SiO_2, hexane–20% EtOAc); (*ii*) 10% yield, CH_2Cl_2, Ar, pyrrole, *p*-tolualdehyde, TFA, 30 min; chloranil, col. chromat. (SiO_2, CH_2Cl_2–50% hexane); (*iii*) 70% yield, THF–CH_3CN–H_2O, $AgNO_3$, NCS, col. chromat. (SiO_2, CH_2Cl_2–0.5% MeOH); (*iv*) 80% yield, THF, mol. sieves, Ar, $CH_3(CH_2)_5NH_2$, 16 h; diethyl ether–EtOH, $NaBH_4$, 3 h, col. chromat. (SiO_2, CH_2Cl_2–5% MeOH); (*v*) 91% yield, CH_2Cl_2, $ZnOAc_2 \cdot H_2O$/MeOH, 10 h, col. chromat. (SiO_2, CH_2Cl_2–5% MeOH); (*vi*) 80% yield, anhydr. THF, MeI, anhydr. K_2CO_3, col. chromat. (SiO_2, CH_2Cl_2–5% MeOH); (*vii*) ion exchange col. chromat. (BF_4^-–IRA96, CH_3CN).

was achieved in MeOH–CH_2Cl_2 using zinc acetate to produce a zinc porphyrin–ferrocene intermediate **2**.[8] Finally, The amine "tail" of **2** was quaternized in anhydrous THF using an excess of methyl iodide to afford $[\mathbf{1}]^+ \cdot I^-$ in 80% yield. The latter was then submitted to ion exchange using a resin in its BF_4^- form to yield $[\mathbf{1}]^+ \cdot BF_4^-$.

NMR characterization

The ^1H NMR spectrum of **2** recorded in $CDCl_3$ [Fig. 2(A)] evidences the coordination of the amine "tail" on a porphyrin metal centre, resulting in five broad, poorly resolved, signals observed at high field between 0 and −5 ppm, reflecting the effect of the porphyrin ring current on the coordinated amine fragment.

These NMR features are a clear consequence of a self-assembly phenomenon that has been presented in a previous communication.[8] This association process could indeed be further characterized from vapour pressure osmometry measurements performed in toluene at 60 °C in the 5–15 × 10^{-3} M concentration range, which yielded an effective molecular weight of 1957 ± 30 in full accordance with a dimeric structure. In agreement with the relative weakness of the secondary amine nitrogen zinc bond, the use of a coordinating NMR solvent such as deuterated DMSO induced the cleavage of this self-assembled structure, as proven by the shift of all the ^1H NMR signals above 0 ppm.

Most of the ^1H NMR signals observed on the spectrum of **2** recorded in non-coordinating $CDCl_3$ were assigned using ^1H–^1H and ^1H–^{13}C correlation spectroscopies. Although the broadest ^1H NMR signals: *e*, *f*, *g* and *h* [Fig. 2(A)], did not exhibit ^1H–^{13}C cross peaks in the HMQC map, their attribution could be achieved from ^1H–^1H correlation experiments that in particular revealed the successive vicinal coupling throughout the hexyl chain (see ESI). Moreover, considering the lack of cross peaks in the ^1H–^1H correlation map involving the signal observed at *ca.* −5 ppm and its disappearance upon addition of D_2O, this signal was attributed to the –NH– proton, which logically is strongly affected by the porphyrin-based anisotropic shielding cone. Surprisingly, even the ferrocene protons were seen to be significantly shifted and were observed between 2.1 and 5 ppm. Assuming that the ring current effect strongly depends on the distance between the porphyrin and a given proton, the ferrocene signal observed at 2.1 ppm was attributed to the closest proton to the coordinated amine fragment [Fig. 2(A), proton *h*]. On the other hand, 1D NOE difference experiments allowed us to evidence through-space interactions between the more deshielded β-pyrrole proton and a ferrocene hydrogen atom located on the Cp ring directly linked to the porphyrin [Fig. 2(B), proton *k*].

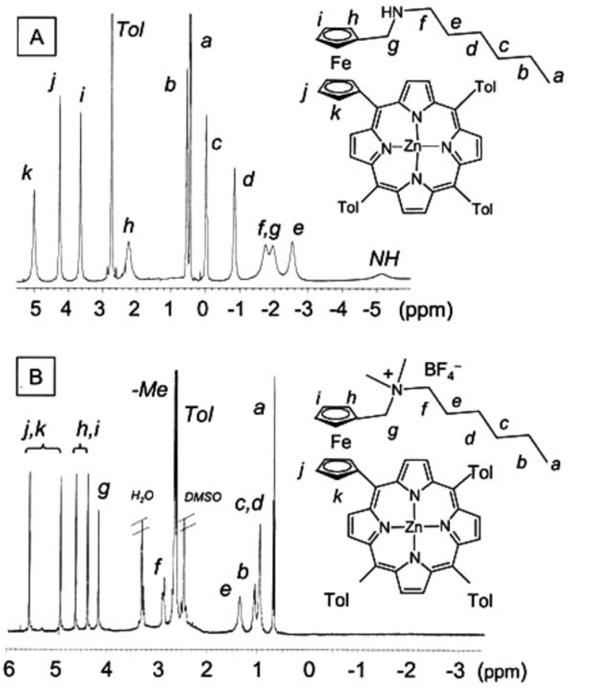

Fig. 2 Part of the ^1H NMR spectra of (A) **2** ($CDCl_3$, 500 MHz) and (B) $[\mathbf{1}]^+ \cdot BF_4^-$ (DMSO–d_6, 400 MHz).

As expected and proven by the ^1H NMR spectrum of $[\mathbf{1}]^+ \cdot BF_4^-$, the quaternization of the hexylamine "tail" induced the cleavage of the self-assembled supramolecular structure. In both non-coordinating ($CDCl_3$) and coordinating (DMSO-d_6) solvents no signals were observed below 0 ppm, reflecting the suppression of the amine's coordinating ability towards the metalloporphyrin centre [Fig. 2(B)]. As a result, all the signals attributed to the hexyl chain logically appeared between 0.5 and 1.5 ppm and the ferrocene signals were observed between 4.2 and 5.6 ppm.

Electrochemical sensing of anions

Cyclic (CV), rotating disk electrode (RDE) and differential pulsed (DPV) voltammetry investigations carried out on $[\mathbf{1}]^+ \cdot BF_4^-$ in CH_2Cl_2 containing 0.1 M TBAP revealed three one-electron reversible oxidation processes [Fig. 3(A,B); also see Fig. 5(C) below] at $E_{1/2}$ = 645, 940 and 1200 mV {*vs.* $[Fe(Cp^*)_2]^{0/+}$; $Fe(Cp^*)_2$ = bis(pentamethylcyclopentadienyl) iron}.

In accordance with previous studies on ferrocene–porphyrin derivatives,[9] the first process was attributed to the ferrocene/ferrocenium couple, followed by two consecutive oxidations of the metalloporphyrin, known to afford successively a radical cation and a dicationic species.[10] Such a well-defined electrochemical signature turned out to strongly contrast with that of the amine precursor **2**. Indeed, the electrochemical features of the latter showed up to five distinct oxidation processes

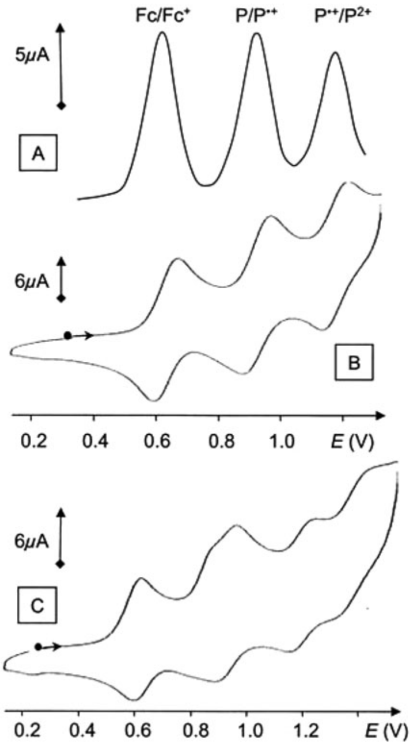

Fig. 3 Differential pulsed (A) and cyclic (B) voltammograms of a 5×10^{-4} M CH_2Cl_2 (TBAP, 0.1 M) solution of $[\mathbf{1}]^+$, BF_4^-; (C) cyclic voltammogram of a 5×10^-4 M CH_2Cl_2 (TBAP, 0.1 M) solution of **2**; 3 mm diameter carbon working electrode; ν = 100 mV s^{-1} (CV) and 10 mV s^{-1} (DPV); E(V) *vs.* $[Fe(Cp^*)_2]^{0/+}$.

[Fig. 3(C)]: a reversible ferrocene-based oxidation at $E_{1/2}$ = 580 mV {*vs.* $[Fe(Cp^*)_2]^{0/+}$}, followed by four porphyrin-based oxidations at E_{pa} = 880 (shoulder), 960, 1240 and 1440 mV {*vs.* $[Fe(Cp^*)_2]^{0/+}$]. As already observed for polymeric structures,[11] the shoulder at 880 mV on the first porphyrin oxidation wave can been attributed to interactions between the porphyrin rings in the supramolecular assembly. The second porphyrin-based irreversible oxidation at 1240 mV leads then to an electrophilic species known to irreversibly lead to isoporphyrins in the presence of nucleophiles.[12] The last oxidation process at 1440 mV thus most presumably results from the oxidation of an isoporphyrin cation wherein the nitrogenous "tail" has been incorporated into the porphyrin framework.

Upon quaternization to form $[\mathbf{1}]^+$, the complex electroactivity of **2** thus evolved into three well-defined reversible redox systems, accompanied by a shift towards more positive potential values of the ferrocene redox couple, directly influenced by the electron-withdrawing character of the ammonium. On the other hand, the overall simplification of the cyclic voltammogram further shows that the complex oxidation pattern observed for **2** arises from the nucleophilic characteristic of the amine, leading to interactions between the porphyrin rings and to isoporphyrin formation.

When increasing amounts of selected anions were added to a solution of $[\mathbf{1}]^+ \cdot BF_4^-$ (5×10^{-4} M in CH_2Cl_2 + 0.1 M TBAP), both ferrocene and porphyrin oxidation processes initially observed at 645 and 938 mV, respectively, underwent significant negative potential shifts. The advantage associated with such a multi-redox detection is clearly put forward when considering the recognition of HSO_4^- and NO_3^-. In both cases, the progressive ferrocene-based potential shifts, induced upon adding tetrabutylammonium hydrogensulfate or nitrate and measured using differential pulsed voltammetry, turned out to be almost identical [Fig. 4(A), $\Delta E \approx -80$ mV after adding 20 molar equivalents of anion].

These changes in the redox potential of the ferrocene centre, which retains quasi-reversible features throughout the electrochemical titration, strongly suggest similar ion pairing effects between the doubly charged ferricinium–ammonium fragment and these anionic species. In contrasts, the stronger basicity of HSO_4^- was clearly evidenced by the significant differences observed in the porphyrin-based electrochemical response. Using the same methodology, the negative potential shift of the first porphyrin-based oxidation peak indeed allowed us to differentiate both anionic species since it reached –140 and −90 mV when 20 molar equivalents of HSO_4^- and NO_3^- were added, respectively.

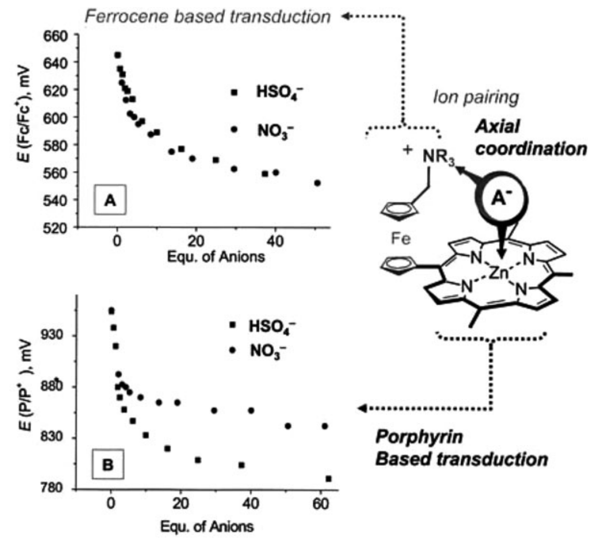

Fig. 4 Evolution of (A) the ferrocene-based and (B) the porphyrin-based DPV oxidation peak potentials for $[\mathbf{1}]^+ \cdot BF_4^-$ (5×10^{-4} M) as a function of added molar equivalents of $TBANO_3$ and $TBAHSO_4$.

Interestingly, as proven by rotating disk electrode measurements, the initial one-electron porphyrin-based oxidation wave, attributed to the $P/P^{+\bullet}$ redox couple, evolved into a two-electron oxidation process upon adding an excess of anionic species. A careful analysis of the electrochemical data revealed the progressive decrease of the $P^{+\bullet}/P^{2+}$ oxidation signal, along with the growth of a new system overlapping the first porphyrin-based oxidation wave (Fig. 5).

It is noteworthy that a similar overlap, which resulted in the observation of only one porphyrin-based oxidation wave in the accessible anodic potential range, was also observed when the electrochemical study of $[\mathbf{1}]^+ \cdot BF_4^-$ was performed in a nucleophilic solvent like DMSO (0.1 M TBAP). Such features, already observed for basket handle and picket fence porphyr-

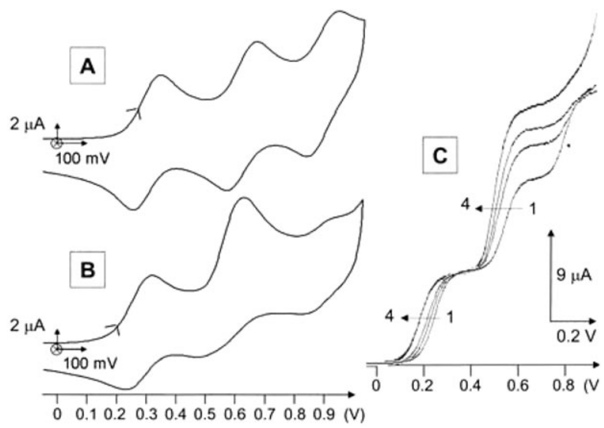

Fig. 5 (A) Cyclic voltammogram of a 5×10^{-4} M CH_2Cl_2 (TBAP, 0.1 M) solution of $[\mathbf{1}]^+ \cdot BF_4^-$. (B) Cyclic voltammogram of a 5×10^{-4} M CH_2Cl_2 (TBAP, 0.1 M) solution of $[\mathbf{1}]^+ \cdot BF_4^-$ + 1 equiv. of $TBANO_3$. (C) Evolution of the RDE curve as a function of added $TBANO_3$: (curve 1) 0, (curve 2) 0.5, (curve 3) 1, (curve 4) 5 equiv. of $TBANO_3$.

ins,[13] strongly suggest the existence of an ECE-type mechanism in which the reaction of the electrogenerated porphyrin-based radical cation with a nucleophilic species would produce a new species that is oxidized at the same or lower potential as the initial $P/P^{+\bullet}$ redox couple. CV experiments performed throughout the electrochemical titration with nitrate and hydrogensulfate revealed that such a coalescence phenomenon was occurring with a significant loss of reversibility in the porphyrin-based oxidation process. A specific sensing of both anionic substrates could nevertheless be achieved through the significant modifications in the porphyrin-based electrochemical activity monitored using differential pulsed voltammetry [Fig. 4(B), porphyrin-based transduction].

A very important perturbation in the electrochemical features of $[\mathbf{1}]^+$ was observed upon addition of dihydrogenphosphate anions, which resulted in a negative shift of the Fc/Fc^+ redox couple up to −240 mV in the presence of 20 molar equivalents of $H_2PO_4^-$. However, the electrochemical recognition properties of $[\mathbf{1}]^+$ towards this anion could not be accurately assessed and compared to the other species, since these changes in electroactivity proceeded with significant loss of reversibility in both ferrocene- and porphyrin-based oxidation waves. Such a behaviour, already observed in the case of simple ferrocene–ammonium probes,[4] puts forward the strong ion pairing effect between $H_2PO_4^-$ and oxidized ferrocenyl receptors that frequently leads to adsorption phenomena.

In contrast, the quasi-reversible features of the ferrocene-based wave in the presence of chloride anions allowed a clear and efficient amperometric-type redox sensing.[14] Using differential pulse voltammetry, the addition of increasing amounts of tetrabutylammonium chloride to a dichloromethane solution of $[\mathbf{1}]^+ \cdot BF_4^-$ led to the progressive decrease of the initial ferrocene-based DPV peak at E_p = 645 mV, along with the growth at a less negative potential of a new peak (E_p = 515 mV, ΔE = −130 mV) corresponding to the complexed receptor [Fig. 6(A)]. The initial wave corresponding to the free ligand completely disappeared and the new peak reached full development after the addition of 1 molar equivalent of chloride anions. This behaviour starkly contrasts with the potentiometric-type "one-wave" redox sensing observed with the rare ferrocene-appended tetraaminophenylporphyrin based chemosensors reported to date.[15]

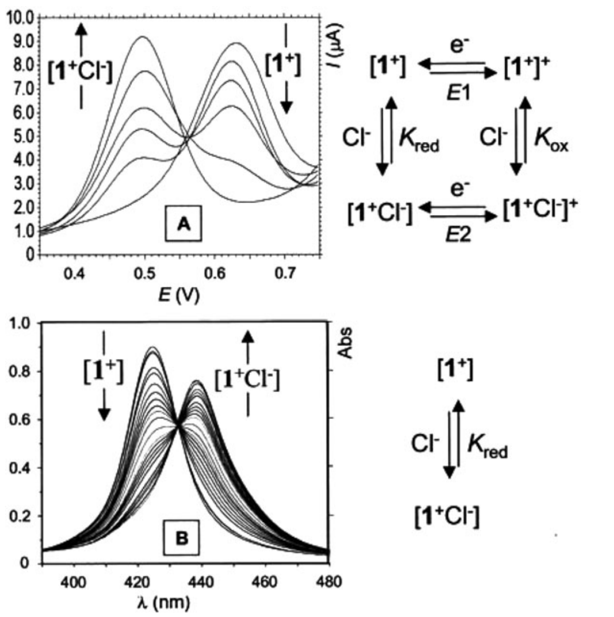

Fig. 6 Evolution of (A) the DPV peak (scan rate 10 mV s^{-1}, same conditions as in Fig. 3) and (B) the Soret visible absorption band (4.8 × 10^{-6} M, CH_2Cl_2, 0.1 M TBAP) of $[\mathbf{1}]^+ \cdot BF_4^-$ as a function of added chloride (0 to 1 and 0 to 500 equiv. for A and B, respectively). The equilibria involved in these evolutions are depicted to the right of the titration curves.

The cumulative effect of multiple anchoring points was revealed by studying independently both fragments constituting $[\mathbf{1}]^+ \cdot BF_4^-$: (i) ferrocene–ammonium and (ii) ferrocene–porphyrin receptors, which did not show such a well-defined "two-wave" behaviour in the presence of chloride anions. As an example, the ferrocene-based oxidation waves of $[Fc–CH_2–N^+(CH_3)_2–(CH_2)_{11}–CH_3] \cdot BF_4^-$ and 5-ferrocenyl-10,15,20-tri (*p*-tolyl)porphyrin underwent only limited potential shifts ($0 \leq -\Delta E \leq 50$ mV) upon addition of 1 equiv. of TBACl. Given the small amplitude of these shifts, the well-behaved two-wave recognition process detailed above can thus be regarded as resulting from the cooperative effect of both binding fragments connected to the same ferrocene redox probe.

Spectrophotometric titration performed on $[\mathbf{1}]^+ \cdot BF_4^-$ in CH_2Cl_2 + 0.1 M TBAP solution resulted in a bathochromic shift, accompanied by a well-defined isosbestic point of the Soret, α and β bands observed in the visible spectra. Analysis of the new Soret band absorbance as a function of added chloride [Fig. 6(B)] was consistent with the formation of a 5-coordinate complex with an estimated stability constant $K_{red}[\mathbf{1}^+ \cdot Cl^-] = 10^4$ M^{-1}, which turns out to be 40 times higher than that obtained in the same conditions with ZnTTP used as a reference ($K_{eq}[ZnTTPCl^-] = 2.5 \times 10^2$ M^{-1}).[16] $K_{red}[\mathbf{1}^+ \cdot Cl^-]$, combined with the potential shift measured upon complexation, allowed us to determine the stability constant $K_{ox}[\mathbf{1}^{2+} \cdot Cl^-]$ of the complex formed between the oxidized ferrocenium form of the receptor and the chloride anion, which is essential to fully account for the specific electrochemical response detailed above (see on Fig. 6 the upper scheme summarizing redox and complexation equilibria for the $[\mathbf{1}]^+ + Cl^-$ system).[17] The magnitude of $K_{ox}[\mathbf{1}^{2+} \cdot Cl^-]$, estimated at 1.7×10^6 M^{-1}, not only explains the specific chloride sensing but also clearly highlights the beneficial effect of oxidation processes in anionic electrochemical recognition. The *in situ* generation of cationic species strongly enhances the binding strength through the reinforcement of electrostatic forces between the anionic species and the oxidized receptor. The anion-sensing properties of $[\mathbf{1}]^+$ proved further to be halide specific since a clear "two-wave" behaviour was also observed in the presence of increasing amounts of $TBA^+ \cdot Br^-$ or $TEA^+ \cdot F^-$, with new waves growing at a less positive potential for fluoride (ΔE = −152 mV) than for bromide (ΔE = −112 mV), in accordance with their relative basicity. These anion-specific potential shifts can be directly related to the halides' relative binding strengths measured by spectrophotometric titration.[18] In the same conditions as in Fig. 6(B) (CH_2Cl_2, 0.1 M TBAP), the stability constant of $[\mathbf{1}^+ \cdot Br^-]$ could be estimated as $K_{red} = 2.5 \times 10^2$ M^{-1}, which is in full agreement with a weaker binding of bromide than chloride for which $K_{red}[\mathbf{1}^+ \cdot Cl^-]$ reached 10^4 M^{-1}.

Conclusion

In conclusion, we have synthesized an ammonium–ferrocene–metalloporphyrin chemosensor allowing a sensitive assessment of the anion's electrostatic and nucleophilic features. The well-defined electrochemical signature associated with a strong reinforcement of the anion binding properties upon oxidation, which produces up to three additional positive charges delocalized throughout the receptor, turns out to be especially suited to achieve efficient electrochemical sensing of anionic species.

The direct connection between the ferrocenyl–ammonium and the metalloporphyrin's π-electronic network, coupled to the cumulative effect of multiple anchoring points, allowed an unprecedented ferrocene-based "two-wave"-type electrochemical sensing of halide anions. Such behaviour, based on ion pairing effects and metal–ligand binding, emphasizes the importance of conjugating complementary interactions and reporting centres.

Due to the ease of modification and versatile properties of both ferrocene and porphyrin fragments, molecular materials based on their intimate association hold great promise in the field of molecular electrochemical recognition. We are currently investigating related molecular architectures that could lead us to achieve challenging redox sensing of exogenic substrates in aqueous media.

Experimental

Reagents, instrumentation and procedures

Prior to use dichloromethane and THF (synthesis grade) were distilled over calcium hydride and Na/benzophenone, respectively. Tetra-*n*-butylammonium perchlorate (TBAP) was purchased from Fluka and used as received. TBAP used for the spectrophotometric titration was obtained from Southwestern Analytical Chemicals and dried under vacuum at 60 °C. Tetra-*n*-butylammonium chloride (>99%), bromide (>98%) and phosphate monobasic (>99%) were obtained from Fluka and used as received. Tetra-*n*-butylammonium hydrogensulfate (>97%) and nitrate (>97%) were obtained from Aldrich and used as received. Tetraethylammonium fluoride dihydrate (>97%) was obtained from Interchim and dried under vacuum at 40 °C before use. Pyrrole and *p*-tolualdehyde were purchased from Aldrich and used as received. 1,1′-Diformyl ferrocene (**7**),[6] 1-[2-(1,3-dithiolanyl)]-1′-formylferrocene (**6**),[7] 1-dodecanaminium, *N*-(ferrocenylmethyl)-*N,N*-dimethyl BF_4^- salt[19] and 5-ferrocenyl-10,15,20-tri(*p*-tolyl)porphyrin[20] were synthesized according to literature procedures.

Molecular sieves were activated by heating at 200 °C under vacuum for 1 h. Electrochemical experiments were conducted with a CHI 660B electrochemical analyzer (CH instrument) in a conventional three-electrode cell under an argon atmosphere at 20 °C. All potentials were referenced to the $[Fe(Cp^*)_2]^{0/+}$ redox couple whose half-wave potential relative to an Ag/$AgNO_3$ reference electrode (10 mM in CH_3CN containing 0.1 M TBAP) is −350 mV. Rotating disc electrode (RDE) voltammetry was carried out at a rotation rate of 600 rpm. Cyclic voltammetry (CV) curves were recorded at a scan rate of 0.1 V s^{-1} and the differential pulse voltammetry (DPV) curves were recorded at a 10 mV s^{-1} scan rate with a pulse height of 25 mV and a step time of 0.2 s. The working electrode was a vitreous carbon disc (3 mm in diameter) polished with 1 μm diamond paste before each recording. ESI (positive mode) mass spectra were recorded with a Bruker Esquire 3000 Plus ion trap spectrometer. FAB (positive mode) mass spectra were recorded with an AEI Kratos MS 50 spectrometer fitted with an Ion Tech Ltd gun and using *m*-nitrobenzyl alcohol as matrix. MALDI-TOF spectra were obtained with a Bruker autoflex using ditranol as matrix (dried drop). NMR spectra were recorded at 25 °C on Bruker AC 250, Bruker Advance 400 MHz or Varian Unity Plus 500 MHz spectrometers. ^1H chemical shifts (ppm) were referenced to residual solvent peaks. UV-Vis spectra were recorded on a Varian Cary 100 spectrophotometer using quartz cells (l = 1 cm). Elemental analyses were performed by the Service Central d'Analyses, CNRS, Lyon.

Syntheses

5-{1′-[2-(1,3-Dithiolanyl)]ferrocenyl}-10,15,20-tri(*p*-tolyl)porphyrin (5). Samples of pyrrole (219 μl, 3.14 mmol), *p*-tolualdehyde (279 μl, 2.35 mmol) and **6** (250 mg, 0.78 mmol) were dissolved in 80 ml of dry CH_2Cl_2 at room temperature in a 150 ml round-bottom flask fitted with a vented rubber septum and flushed for 15 min with argon. The mixture was then protected from light and trifluoroacetic acid (121 μl, 1.57 mmol) was slowly added under vigorous stirring. The resulting solution was stirred at room temperature for 30 min, then 2,4,6-collidine (209 μl, 1.57 mmol) was added, followed by chloranil (385 mg, 1.56 mmol). The mixture was stirred at room temperature for 3 h and brought to dryness under reduced pressure. One hundred millilitres of an aqueous NaOH solution (2 M) were added to the oily residue and the mixture was stirred at room temperature for 1 h. The black precipitate was then filtered, washed with water and dried under reduced pressure. The mixture was then purified by chromatography (SiO_2, CH_2Cl_2–hexane 75 : 25) to yield **5** (74 mg, 10%) as a black-green solid. MS (FAB): m/z 869 $[M + 1]^+$; NMR ^1H ($CDCl_3$, 500 MHz): δ −2.35 (s, 2H, –NH–), 2.71 (s, 3H, –Me), 2.73 (s, 6H, –Me), 3.15–3.33 [m, 4H, $–S(CH_2)_2S–$], 4.11 (m, 2H, –Fc), 4.38 (m, 2H, –Fc), 4.90 (m, 2H, –Fc), 5.53 (s, 1H, $–HCS–)_2$), 5.59 (m, 2H, –Fc), 7.56 (m, 6H, –Tol), 8.10 (m, 6H, –Tol), 8.83 (m, 6H, β-pyrr, –Tol), 9.95 (d, ^3J = 4.90 Hz, 2H, β-pyrr); $\lambda_{max}(CH_2Cl_2)$/nm: 422 (S), 510 (Q), 588 (Q), 671 (Q); anal. calcd. for $C_{54}H_{44}FeN_4S_2$: C 74.64, H 5.10, N 6.45%; obs. C 74.41, H 5.18, N 6.44%.

5-[1′-(Formyl)ferrocenyl]-10,15,20-tri(*p*-tolyl)porphyrin (4). **5** (50 mg, 5.7×10^{-5} mol) dissolved in 50 ml of THF was quickly added to a solution of *N*-chlorosuccinimide (56 mg, 0.42 mmol) and silver nitrate (54.5 mg, 0.32 mmol) in 35 ml of CH_3CN–H_2O (85 : 15). After stirring at room temperature for 10 min, 1 ml of saturated aqueous Na_2SO_3 solution was added, followed by successive addition of saturated Na_2CO_3 (1 ml) and brine (1 ml). Fifty millilitres of dichloromethane were then added and the resulting mixture was filtered. After washing the solid residue with dichloromethane, the organic phases were combined, washed with water and dried over anhydrous Na_2SO_4. The black powder obtained after evaporation under reduced pressure was purified by chromatography (SiO_2, CH_2Cl_2–MeOH 99 : 1) to yield **4** (32 mg, 70%) as a purple solid. MS (FAB): m/z 793 $[M + 1]^+$; NMR ^1H ($CDCl_3$, 250 MHz): δ −2.36 (br s, 2H, –NH–), 2.67 (s, 3H, –Me), 2.69 (s, 6H, –Me), 4.44 (m, 2H, –Fc), 4.83 (m, 2H, –Fc), 4.92 (m, 2H, –Fc), 5.59 (m, 2H, –Fc), 7.51–7.56 (m, 6H, –Tol), 8.03–8.08 (m, 6H, –Tol), 8.74–8.82 (m, 6H, β-pyrr), 9.81 (d, 2H, ^3J = 4.8 Hz, β-pyrr), 9.90 (s, 1H, –CHO); $\lambda_{max}(CH_2Cl_2)$/nm: 423 (S), 528 (Q), 576 (Q), 600 (sh), 666 (Q).

5-[1′-(Hexylaminomethyl)ferrocenyl]-10,15,20-tri(*p*-tolyl)porphyrin (3). **4** (150 mg, 0.19 mmol) and hexylamine (30 μl, 0.22 mmol) were added to an argon-flushed 50 ml round-bottom flask containing 20 ml of anhydrous THF and activated molecular sieves. The resulting mixture was stirred at room temperature under argon for 16 h, filtered to remove the molecular sieves, which were washed well with anhydrous THF, and finally concentrated under reduced pressure. After adding $NaBH_4$ (63 mg, 1.66 mmol) dissolved in absolute ethanol, the solution was stirred at room temperature for 3 h and evaporated to dryness. The resulting crude solid was dissolved in 50 ml of dichloromethane and washed with water. The organic phase was dried over anhydrous sodium sulfate, filtered and evaporated to afford a crude product, which was purified by chromatography (SiO_2, CH_2Cl_2–MeOH 99 : 1) to yield **3** (132 mg, 80%). MS (FAB): m/z 878 $[M + 1]^+$; NMR ^1H ($CDCl_3$, 250 MHz): δ −2.33 (s, 2H, NH), 0.50–0.90 (m, 11H, –hexyl), 2.08 (m, 2H, $NHCH_2CH_2$–), 2.66 (s, 3H, –Me), 2.69 (s, 6H, –Me), 3.29 (br s, 2H, $–FcCH_2–$), 4.09 (br s, 2H, –Fc), 4.22 (br s, 2H, –Fc), 4.73 (br s, 2H, –Fc), 5.48 (br s, 2H, –Fc), 7.53–7.56 (m, 6H, –Tol), 8.05–8.09 (m, 6H, Tol), 8.75–8.80 (m, 6H, β-pyrr), 9.94 (d, 2H, ^3J = 4.8 Hz, β-pyrr); $\lambda_{max}(CH_2Cl_2)$/nm (log ε): 422 (5.56) (S), 512 (4.09) (Q), 598 (3.98) (Q), 673 (3.97) (Q).

Zinc(II) 5-[1′-(hexylaminomethyl)ferrocenyl]-10,15,20-tri (*p*-tolyl)porphyrin (2). One millilitre of methanol saturated with zinc(II) acetate was added to **3** (50 mg, 0.56 × 10^{-4} mol) dissolved in 20 ml of dichloromethane. The resulting mixture was stirred at room temperature for 10 h. This solution was then washed with water, dried over anhydrous sodium sulfate, filtered and evaporated to dryness. The crude product was then purified by chromatography (SiO_2, CH_2Cl_2–MeOH 99 : 1) to yield **2** (48 mg, 91%). MS (MALDI-TOF): m/z 939.2 $[M]^+$; ^1H NMR ($CDCl_3$, 500 MHz, 293 K): δ −5.18 (br s, 1H), −2.54 (br s, 2H), −1.98 (br s, 2H), −1.76 (br s, 2H), −0.86 (br s, 2H), −0.03 (br s, 2H), 0.43 (t, $^3J = 7$ Hz, 3H, –CH_2CH_3), 0.52 (m, 2H, –CH_2CH_3), 2.23 (br s, 2H, –Fc), 2.72 (s, 3H, –$PhCH_3$), 2.73 (s, 6H, –$PhCH_3$), 3.64 (br s, 2H, –Fc), 4.24 (br s, 2H, –Fc), 5.0 (br s, 2H, –Fc), 7.53–7.60 (m, 6H), 8.07–8.15 (m, 6H), 8.87 (m, 6H), 9.82 (br s, 2H, β-pyr); ^{13}C NMR ($CDCl_3$, 62.5 MHz, 293 K): δ 13.5, 21.5, 22.0, 23.9, 24.9, 30.2, 42.8, 42.9, 69.4, 69.5, 71.0, 78.2, 82.5, 90.7, 116.1, 120.2, 120.9, 127.1, 130.7, 131.4, 131.5, 134.3, 134.7, 136.7, 140.2, 140.4, 149,2, 149.8, 150.0, 150.2; $\lambda_{max}(CH_2Cl_2)$/nm (log ε): 429 (5.43), 580 (4.06), 631 (4.28); anal. calcd. for $C_{58}H_{53}FeN_5Zn$: C 74.00, H 5.67, N 7.44%; obs. C 73.15, H 5.66, N 7.30%.

Zinc(II) [5-{1′-(methanaminium,*N*-hexyl-*N*,*N*-dimethyl)ferrocenyl}-10,15,20-tri(*p*-tolyl)porphyrin]tetrafluoroborate (1). Anhydrous K_2CO_3 (12.8 mg, 7.87 × 10^{-5} mol) and **2** (74.1 mg, 6.44 × 10^{-5} mol) were placed under an argon atmosphere in a 25 ml round-bottom flask, fitted with a rubber septum. Twelve millilitres of anhydrous THF were then added with a syringe, followed by methyl iodide (366 μl, 5.87 mmol). The resulting mixture was stirred at room temperature for 24 h and then filtered. The solid was washed with THF and the solution was concentrated under reduced pressure to give a green crude solid, which was purified by chromatography (SiO_2, CH_2Cl_2–MeOH 95 : 5) to afford $[\mathbf{1}]^+ \cdot I^-$ (69 mg, 80%). The latter was then submitted to ion exchange chromatography using an IRA-96 resin first conditioned with a 40% HBF_4 aqueous solution and washed well with water and acetonitrile. $[\mathbf{1}]^+ \cdot I^-$ was dissolved in acetonitrile and passed through the resin to obtain quantitatively $[\mathbf{1}]^+ \cdot BF_4^-$. MS (ESI+): m/z 968.6 $[M]^+$; ^1H NMR [$(CD_3)_2SO$, 400 MHz, 293 K]: δ 0.72 (t, $^3J = 7.2$ Hz, 3H, –CH_2CH_3), 0.99 (m, 4H, –CH_2–), 1.09 (m, 2H, –CH_2–), 1.39 (m, 2H, –CH_2–), 2.65 (s, 3H, –CH_3), 2.68 (s, 6H, –CH_3), 2.70 (s, 6H, –CH_3), 2.90 (m, 2H, –NCH_2CH_2–), 4.20 (s, 2H, –N^+–CH_2Fc), 4.42 (m, 2H, –Fc), 4.65 (m, 2H, –Fc), 4.96 (m, 2H, –Fc), 5.58 (m, 2H, –Fc), 7.57–7.61 (m, 6H), 8.00–8.04 (m, 6H), 8.68–8.72 (m, 4H), 8.78 (d, $^3J = 4.8$ Hz, 2H, β-pyr), 10.04 (m, 2H, β-pyr); $\lambda_{max}(CH_2Cl_2)$/nm (log ε): 424 (5.48) (S), 563 (4.19) (Q), 610 (4.09) (Q); anal. calcd. for $C_{60}H_{58}BF_4FeN_5Zn \cdot H_2O$: C 67.02, H 5.62, N 6.51%; obs. C 67.04, H 5.50, N 6.52%.

References

1 (*a*) P. D. Beer and P. A. Gale, *Angew. Chem., Int. Ed.*, 2001, **40**, 486; (*b*) P. D. Beer and E. J. Hayes, *Coord. Chem. Rev.*, 2003 **240**, 167.

2 (*a*) H.-J. Schneider, *Angew. Chem., Int. Ed. Engl.*, 1991, **30**, 1417; (*b*) F. P. Schmidten and M. Berger, *Chem. Rev.*, 1997, **97**, 1609; (*c*) M. M. Antonisse and D. N. Reinhoudt, *Chem. Commun.*, 1998, 443.

3 For ferrocenyl directly linked to a porphyrin, see: (*a*) R. G. Wollmann and D. N. Hendrickson, *Inorg. Chem.*, 1977, **16**, 3079; (*b*) N. M. Loim, N. V. Abramova and V. I. Sokolov, *Mendeleev Commun.*, 1996, 46; (*c*) N. M. Loim, N. V. Abramova, R. Z. Khaliullin and V. I. Sokolov, *Russ. Chem. Bull.*, 1997, **46**, 1193; (*d*) N. M. Loim, N. V. Abramova, R. Z. Khaliullin, Y. S. Lukashov, E. V. Vorontsov and V. I. Sokolov, *Russ. Chem. Bull.*, 1998, **47**, 1016; (*e*) V. A. Nadtochenko, N. N. Denisov, V. Y. Gak, N. V. Abramova and N. M. Loim, *Russ. Chem. Bull.*, 1999, **48**, 1900; (*f*) P. D. W. Boyd, A. K. Burrell, W. M. Campbell, P. A. Cocks, K. C. Gordon, G. B. O. Jameson, D. L. Officer and Z. Zhao, *Chem. Commun.*, 1999, 637; (*g*) S. W. Rhee, B. B. Park, Y. Do and J. Kim, *Polyhedron*, 2000, **19**, 1961; (*h*) S. W. Rhee, Y. H. Na, Y. Do and J. Kim, *Inorg. Chim. Acta*, 2000, **309**, 49; (*i*) S. J. Narayanan, S. Venkatraman, S. R. Dey, B. Sridevi, V. R. G. Anand and T. K. Chandrashekar, *Synlett.*, 2000, **12**, 1834; (*j*) H. J. H. Wang, L. Jaquinod, D. J. Nurco, M. G. H. Vicente and K. Smith, *Chem. Commun.*, 2001, 2646; (*k*) V. A. Nadtochenko, D. V. Khudyakov, E. V. Vorontsov, N. M. Loim, F. E. Gostev, D. G. Tovbin, A. A. Titov and O. M. Sarkisov, *Russ. Chem. Bull.*, 2002, **51**, 986.

4 (*a*) O. Reynes, J.-C. Moutet, J. Pécaut, G. Royal and E. Saint-Aman, *New J. Chem.*, 2002, **26**, 9; (*b*) O. Reynes, J.-C. Moutet, G. Royal and E. Saint-Aman, *Electrochim. Acta*, 2004, **49**, 3727.

5 (*a*) J. Weiss, *J. Inclusion Phenom. Macrocyclic Chem.*, 2001, **40**, 1; (*b*) P. D. Beer, D. P. Cormode and J. J. Davis, *Chem. Commun.*, 2004, **4**, 414.

6 G. G. A. Balavoine, G. Doisneau and T. Fillebeen-Khan, *J. Organomet. Chem.*, 1991, **412**, 381.

7 B. Basu, S. K. Chattopadhyay, A. Ritzen and T. Frejd, *Tetrahedron: Asymmetry*, 1997, **8**, 1841.

8 C. Bucher, C. H. Devillers, J.-C. Moutet, G. Royal and E. Saint-Aman, *Chem. Commun.*, 2003, 888.

9 (*a*) E. S. Schmidt, T. S. Calderwood and T. C. Bruice, *Inorg. Chem.*, 1986, **25**, 3718; (*b*) A. K. Burrell, W. M. Campbell, D. L. Officer, S. M. Scott, K. C. Gordon and M. R. McDonald, *J. Chem. Soc., Dalton Trans.*, 1999, 3349; (*c*) A. Arounaguiry, R. W. Wagner, P. D. Rao, J. A. Riggs, P. Hascoat, J. R. Diers, J. Seth, R. K. Lammi, D. F. Bocian, D. Holten and J. S. Lindsey, *Chem. Mater.*, 2001, **13**, 1023.

10 K. M. Kadish, E. Van Caemelbecke and G. Royal, in *The Porphyrin Handbook*, eds. K. M. Kadish, K. M. Smith and R. Guilard, Academic Press, San Diego, CA, 2000, vol. **8**, ch. 55.

11 (*a*) K. Funatsu, T. Imamura, A. Ichimura and Y. Sasaki, *Inorg. Chem.*, 1998, **37**, 1798; (*b*) C. Ikeda, Y. Tanaka, T. Fujihara, Y. Ishii, T. Ushiyama, K. Yamamoto, N. Yoshioka and H. Inoue, *Inorg. Chem.*, 2001, **40**, 3395.

12 (*a*) H. J. Shine, A. G. Padilla and S.-M. Wu, *J. Org. Chem.*, 1979, **44**, 4069; (*b*) K. M. Kadish and R. K. Rhodes, *Inorg. Chem.*, 1981, **20**, 2961; (*c*) A. S. Hinman, B. D. Pavelich, A. E. Kondo and S. Pons, *J. Electroanal. Chem.*, 1987, **234**, 145; (*d*) L. Persaud and C. H. Langford, *Inorg. Chim. Acta*, 1987, **129**, 31.

13 (*a*) Overlapping of porphyrin-based oxidation processes have already been described in the literature. See, for examples: L. Geng and R. W. Murray, *Inorg. Chem.*, 1986, **25**, 3115; (*b*) L. Geng, A. G. Ewing, J. C. Jernigan and R. W. Murray, *Anal. Chem.*, 1986, **58**, 852; (*c*) K. M. Kadish, D. Sazou, G. B. Maiya, B. C. Han, Y. M. Liu, A. Saoiabi, M. Ferhat and R. Guilard, *Inorg. Chem.*, 1989, **28**, 2542; (*d*) A. El-Kasmi, D. Lexa, P. Maillard, M. Momenteau and J.-M. Savéant, *J. Am. Chem. Soc.*, 1991, **113**, 1586; (*e*) J. A. Hodge, M. G. Hill and H. B. Gray, *Inorg. Chem.*, 1995, **34**, 809.

14 Well-behaved redox sensing of halides is of special interest since they frequently undergo catalytic oxidation by ferrocene-based receptors. See: M. Buda, A. Ion, J.-C. Moutet, E. Saint-Aman and R. Ziessel, *J. Electroanal. Chem.*, 1999, **469**, 132 and references therein.

15 (*a*) P. D. Beer, M. G. B. Drew and R. Jagessar, *J. Chem. Soc., Dalton Trans.*, 1997, 881; (*b*) M. C. Hodgson, A. K. Burrell, P. D. W. Boyd, P. J. Brothers and C. E. F. Rickard, *J. Porphyrins Phthalocyanines*, 2002, **6**, 737.

16 This is in full agreement with literature values obtained with ZnTPP in similar conditions: (*a*) M. Nappa and J. S. Valentine, *J. Am. Chem. Soc.*, 1978, **100**, 5075; (*b*) A. S. Hinman and B. D. Pavelich, *J. Electroanal. Chem.*, 1989, **269**, 53.

17 (*a*) R. Miller, D. A. Gutowski, Z. H. Chen, G. W. Gokel, L. Echegoyen and A. E. Kaifer, *Anal. Chem.*, 1988, **60**, 2021; (*b*) P. D. Beer, P. A. Gale and G. Z. Chen, *J. Chem. Soc., Dalton Trans.*, 1999, 1897.

18 Attempts to fit the experimental data obtained upon F^- addition did not lead to satisfactory results.

19 1-Dodecanaminium, *N*-(ferrocenylmethyl)-*N*,*N*-dimethyl Br^- salt was synthesized according to T. Saji, K. Hoshino and S. Aoyagui, *J. Am. Chem. Soc.*, 1985, **107**, 6865 and submitted to anion exchange chromatography using an IRA-96 resin conditioned with a 40% HBF_4 aqueous solution (see synthesis of $[\mathbf{1}]^+ \cdot BF_4^-$).

20 S. J. Narayanan, S. Venkatraman, S. R. Dey, B. Sridevi, V. R. G. Anand and T. K. Chandrashekar, *Synlett.*, 2000, **12**, 1834.